

Improvement of LaBr₃:5%Ce scintillation properties by Li⁺, Na⁺, Mg²⁺, Ca²⁺, Sr²⁺, and Ba²⁺ co-doping

Mikhail S. Alekhin,¹ Daniel A. Biner,² Karl W. Krämer,² and Pieter Dorenbos^{1,a)}

¹Department of RST-FAME, Faculty of Applied Sciences, Delft University of Technology, Mekelweg 15, 2629 JB Delft, The Netherlands

²Department of Chemistry and Biochemistry, University of Bern, Freiestrasse 3, CH-3012 Bern, Switzerland

(Received 24 April 2013; accepted 27 May 2013; published online 12 June 2013)

This paper reports on the effects of Li⁺, Na⁺, Mg²⁺, Ca²⁺, Sr²⁺, and Ba²⁺ co-doping on the scintillation properties of LaBr₃:5%Ce³⁺. Pulse-height spectra of various gamma and X-ray sources with energies from 8 keV to 1.33 MeV were measured from which the values of light yield and energy resolution were derived. Sr²⁺ and Ca²⁺ co-doped crystals showed excellent energy resolution as compared to standard LaBr₃:Ce. The proportionality of the scintillation response to gamma and X-rays of Ca²⁺, Sr²⁺, and Ba²⁺ co-doped samples also considerably improves. The effects of the co-dopants on emission spectra, decay time, and temperature stability of the light yield were studied. Multiple thermoluminescence glow peaks, decrease of the light yield at temperatures below 295 K, and additional long scintillation decay components were observed and related to charge carrier traps appearing in LaBr₃:Ce³⁺ with Ca²⁺, Sr²⁺, and Ba²⁺ co-doping.

© 2013 AIP Publishing LLC. [<http://dx.doi.org/10.1063/1.4810848>]

I. INTRODUCTION

Discovered in 2001 (Ref. 1), LaBr₃:Ce has a unique combination of high light yield of 70 000 photons/MeV, excellent energy resolution of 2.7% at 662 keV, decent proportional response, and short decay time of 15 ns. Owing to these properties, LaBr₃:Ce meets the requirements of numerous applications.^{2,3} For example, the high light output and the excellent time and energy resolution make LaBr₃:Ce a good detector material for time-of-flight positron emission tomography (TOF PET).⁴ A 100 ps coincidence resolving time (CRT) for 511 keV annihilation photon pairs was achieved with a LaBr₃:Ce scintillator in combination with silicon photomultipliers (SiPM).⁵ The high γ -ray detection efficiency and excellent energy resolution in combination with sufficient radiation tolerance⁶ qualified LaBr₃:Ce for the European Space Agency Japan Aerospace Exploration Agency (ESA/JAXA) BepiColombo mission to Mercury.⁷ LaBr₃:Ce is a mechanically robust scintillation material with remarkable light yield at high temperatures, thus a good candidate for online logging in drill heads for oil well prospecting.⁸ The performance of Ø3.5 in. × 6 in. LaBr₃:Ce detectors is very satisfactory for high energy γ -ray measurements.⁹ LaBr₃:Ce has also a potential for the use in scintillation cameras for X-ray and γ -ray imaging.¹⁰

For the majority of the mentioned applications, the energy resolution is a very important parameter, and its further improvement will be very beneficial. Recently, LaBr₃:5%Ce co-doped with Sr showed a record low energy resolution of 2% at 662 keV.¹¹ This improvement was ascribed to a more proportional response of LaBr₃:5%Ce, Sr as compared to standard LaBr₃:5% Ce.¹¹ Yang *et al.*¹² also observed light yield, energy resolution, and proportionality improvements of Sr and Ba co-doped LaBr₃:5%Ce crystals.

However, many important questions remain unanswered, for example, about the origin of these improvements and whether LaBr₃:Ce can be co-doped with other elements to perform even better than LaBr₃:Ce,Sr. Those questions motivated us to grow LaBr₃:Ce crystals with different co-dopants, and study their effect on the scintillation properties and the scintillation mechanism of LaBr₃:Ce.

This work concerns the evaluation of the light yield, energy resolution, non-proportionality, and other scintillation properties of LaBr₃:Ce with 6 different co-dopants: Li⁺, Na⁺, Mg²⁺, Ca²⁺, Sr²⁺, and Ba²⁺. Special attention is paid to an improved energy resolution of Sr co-doped LaBr₃:Ce over the 8 keV–1.33 MeV energy range.

II. EXPERIMENT

A. Crystal growth

LaBr₃:5%Ce crystals were independently grown at two institutes. Those from Saint-Gobain Crystals are referred to as *group A* crystals. They were grown using LaBr₃, 5 mol. % CeBr₃, and 0.35–0.75 mol. % LiBr or SrBr₂ starting materials with a propriety method also used for the commercially available BriLanCe380 standard LaBr₃:5%Ce scintillators. 100–200 atomic ppm of Sr were detected in Sr co-doped LaBr₃:Ce crystalline matrix by Inductively Coupled Plasma (ICP) analysis.

The other crystals, referred to as *group B* crystals, were grown at the University of Bern. Starting from LaBr₃, 5 mol. % CeBr₃, and 0.5 mol. % NaBr, MgBr₂, CaBr₂, SrBr₂, or BaBr₂ crystals were grown by the vertical Bridgman technique from the melt. Irregularly shaped pieces with sizes ranging from 10 to 100 mm³ were cleaved from the original crystal boules for further studies.

Both groups produced the co-doped crystals together with standard LaBr₃:5%Ce for reference. In this work, we refer to

^{a)}Author to whom correspondence should be addressed. Electronic mail: P.Dorenbos@tudelft.nl.

standard $\text{LaBr}_3:5\% \text{Ce}$ as $\text{LaBr}_3:\text{Ce}$ and to $\text{LaBr}_3:5\% \text{Ce}$ co-doped with a further element X as $\text{LaBr}_3:\text{Ce},\text{X}$. No visible differences in crystal quality were observed between the standard and the co-doped samples.

B. Experimental methods

662 keV γ -ray excited pulse-height spectra at room temperature were recorded with a standard bialkali Hamamatsu R1791 photo multiplier tube (PMT) or a super bialkali Hamamatsu R6231-100 PMT connected to a Cremat CR-112 pre-amplifier and an Ortec 672 spectroscopic amplifier with 0.5–10 μs shaping time. The bare crystals were mounted on the window of the PMT and covered with several 0.1 mm thick Teflon layers. Due to very high light yield and short decay time, the peak currents flowing through the PMT might undergo saturation causing non-linearity of the PMT gain.¹³ To avoid this, 400 V cathode voltage was used, and the signal was read from the sixth dynode at ground potential. Due to the hygroscopic nature of $\text{LaBr}_3:\text{Ce}$, all pulse-height measurements were performed inside an M-Braun UNILAB dry box with a moisture level of less than 1 part per million. The light yield expressed in photoelectrons per MeV of absorbed γ -ray energy (phe/MeV) was determined without an optical coupling between the scintillator and the PMT-window. The yield was obtained from the ratio between the peak position of the 662 keV photopeak and the position of the mean value of the so-called single photoelectron peak¹⁴ in pulse-height spectra. Single photoelectron spectra were recorded with a Hamamatsu R1791 PMT connected to a Cremat CR-110 pre-amplifier. The absolute light yield expressed in photons per MeV (ph/MeV) was determined by correcting for the quantum efficiency and reflectivity of the PMT as outlined in Ref. 14. The energy resolution (R) was defined as the Full Width at Half Maximum intensity (FWHM) over the peak position of the photopeak in a pulse-height spectrum.

The non-proportionality (nPR) at an X-ray or γ -ray energy (E_x) was defined as the ratio between the number of photoelectrons per MeV observed at E_x and that observed at 662 keV. nPR was studied with a standard set of radioactive sources (²⁴¹Am, ¹³⁷Cs, ¹³³Ba, ⁶⁰Co, and ²²Na) plus an Amersham variable energy X-ray source.

X-ray excited luminescence and thermoluminescence spectra were recorded using an X-ray tube with Cu anode operating at 60 kV and 25 mA. The emission of the sample was focused via a quartz window and a lens on the entrance slit of an ARC VM504 monochromator (blazed at 300 nm, 1200 grooves/mm), dispersed, and recorded with a Hamamatsu R943-02 PMT. The spectra were corrected for the monochromator transmission and the quantum efficiency of the PMT. X-ray excited luminescence measurements were performed between 80 K and 600 K using a Janis VPF-800 cryostat operated with a LakeShore 331 temperature controller. Due to the high moisture sensitivity of $\text{LaBr}_3:\text{Ce}$ the cryostat was baked out to remove all water from the system prior to sample mounting. The PMT was outside the cryostat and remained always at room temperature. For thermoluminescence measurements, ~ 1 mm thick crystals were pressed by a needle spring to the

bottom of the sample holder inside the cryostat without thermal coupling. The crystals were cooled down to 78 K and then irradiated with the X-rays during 20 min leading to a steady state X-ray excited luminescence (SSL). After switching off the X-rays, the crystals were heated with a rate of 0.1 K/s using a LakeShore 331 temperature controller. The thermoluminescence emission was monitored at 380 nm and measured with a Hamamatsu R943-02 PMT.

Scintillation time profiles were recorded by the delayed coincidence single photon counting method,¹⁵ with a setup described in Ref. 16. A ¹³⁷Cs γ -ray source was used for excitation. The same setup without “stop” PMT was used for temperature dependent pulse-height measurements.

III. RESULTS AND DISCUSSION

The first part of this section is devoted to the light yield and energy resolution of group A $\text{LaBr}_3:\text{Ce},\text{Sr}$ samples, which showed the best performance among the studied crystals. The second part deals with the effects of all the studied co-dopants on the scintillation properties of $\text{LaBr}_3:\text{Ce}$.

A. Light yield and energy resolution of $\text{LaBr}_3:\text{Ce},\text{Sr}$

The light yield of group A $\text{LaBr}_3:\text{Ce},\text{Sr}$ measured at 662 keV with 10 μs amplifier shaping time is 78 000 ph/MeV. It is slightly higher than 76 000 ph/MeV of the standard $\text{LaBr}_3:\text{Ce}$. However, measured with 0.5–3 μs shaping times, the yield of $\text{LaBr}_3:\text{Ce},\text{Sr}$ is lower as compared to $\text{LaBr}_3:\text{Ce}$, see Table I. This is due to additional slow components of the scintillation decay of Sr co-doped $\text{LaBr}_3:\text{Ce}$. As will be shown in Sec. III B, those components have decay time in a range of microseconds.

The energy resolution of Sr co-doped $\text{LaBr}_3:\text{Ce}$ is considerably better as compared to the standard $\text{LaBr}_3:\text{Ce}$. Fig. 1 is from Ref. 11 and shows that the 662 keV full absorption peak improves from 2.45% to 2.04%. Note that this record low value was obtained during 24 h acquisition with ~ 200 000 counts under the photopeak and 1 μs shaping time. Interestingly, varying the shaping time between 0.5 and 10 μs does not change the energy resolution of $\text{LaBr}_3:\text{Ce},\text{Sr}$ at 662 keV by more than 0.05%.

⁶⁰Co pulse-height spectra measured with $\text{LaBr}_3:\text{Ce}$ and $\text{LaBr}_3:\text{Ce},\text{Sr}$ are compared in Fig. 2. The 1.17 MeV (1) and 1.33 MeV (2) full absorption peaks are better resolved in the spectrum of the Sr co-doped sample. One can also clearly distinguish the La- K_α escape peak from the 1.33 MeV peak in the $\text{LaBr}_3:\text{Ce},\text{Sr}$ spectrum.

Even more spectacular improvements were observed at energies below 60 keV. In Ref. 11, we presented the spectrum of ²⁴¹Am. Fig. 3 shows the pulse-height spectra from a

TABLE I. Light yield of group A $\text{LaBr}_3:\text{Ce}$ and $\text{LaBr}_3:\text{Ce},\text{Sr}$ derived from ¹³⁷Cs pulse height spectra measured with various shaping times.

Crystal	Light yield at 662 keV (10^3 ph/MeV)			
	0.5 μs	1 μs	3 μs	10 μs
$\text{LaBr}_3:\text{Ce},\text{Sr}$	68	71	75	78
$\text{LaBr}_3:\text{Ce}$	72	74	75	76

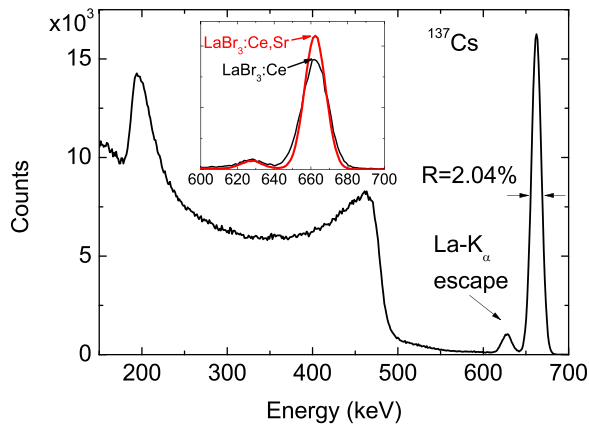


FIG. 1. Pulse-height spectrum of a ^{137}Cs source measured with a group A $3 \times 3 \times 1 \text{ mm}^3$ $\text{LaBr}_3:\text{Ce,Sr}$ crystal and a super bialkali R6231-100 PMT. The inset compares $\text{LaBr}_3:\text{Ce}$ and $\text{LaBr}_3:\text{Ce,Sr}$ 662 keV photo-peaks on an enlarged scale. The peaks are normalized so that the integral numbers of counts below them are equal.

Tb target of the variable energy X-ray source. 44.2 keV K_α Tb X-rays (1), 50.7 keV K_β Tb X-rays (2), and ^{241}Am 59.5 keV γ -rays (3) appear as separate peaks in the $\text{LaBr}_3:\text{Ce,Sr}$ spectrum, while for standard $\text{LaBr}_3:\text{Ce}$ peaks (2) and (3) are observed only as shoulders. (4) and (5) are La K_α , and (6) La K_β escape peaks. They are slightly misaligned in the $\text{LaBr}_3:\text{Ce,Sr}$ spectrum as compared to the $\text{LaBr}_3:\text{Ce}$ spectrum. This is caused by a more proportional response of the $\text{LaBr}_3:\text{Ce,Sr}$ scintillator.¹¹

Table II compiles the values of the energy resolution, which were determined from the full absorption peaks of pulse-height spectra measured with various radioactive sources. The peaks were fitted with single or multiple Gaussian functions depending on the number of closely located energy lines. The only exception were the 8.04 keV K_α and 8.91 keV K_β Cu target lines, which were fitted with a single Gaussian function. $\text{LaBr}_3:\text{Ce,Sr}$ shows on average 25% smaller values of the energy resolution as compared to standard $\text{LaBr}_3:\text{Ce}$ at all the studied energies between 8 keV and 1.33 MeV, see Table II. Whereas $\text{LaBr}_3:\text{Ce}$ shows worse performance compared to NaI:Tl at energies below 100 keV,¹³ the co-doped $\text{LaBr}_3:\text{Ce,Sr}$ outperforms NaI:Tl .

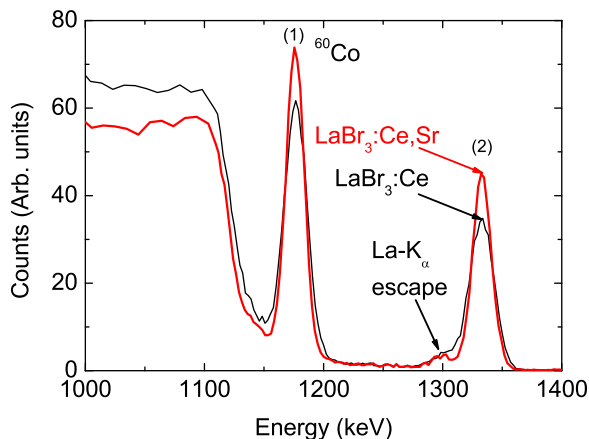


FIG. 2. Pulse-height spectra of a ^{60}Co source measured with group A $\text{LaBr}_3:\text{Ce}$ and $\text{LaBr}_3:\text{Ce,Sr}$ crystals and a R6231-100 PMT. The spectra are normalized so that the integral numbers of counts below the 1.33 MeV photo-peaks are equal.

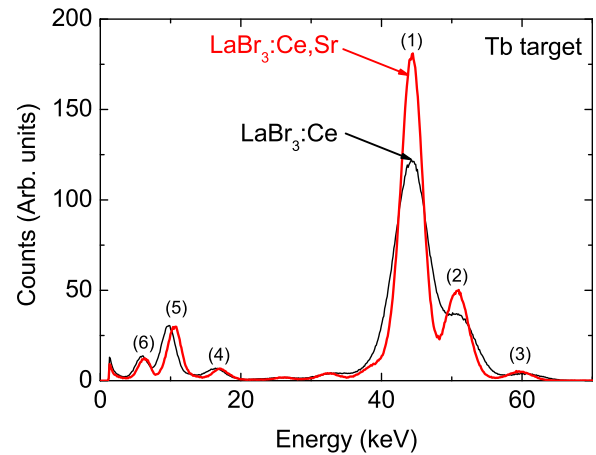


FIG. 3. Pulse-height spectra from a Tb target of the variable energy X-ray source measured with $\text{LaBr}_3:\text{Ce}$ and $\text{LaBr}_3:\text{Ce,Sr}$ crystals and a R6231-100 PMT. The spectra are normalized so that the integral numbers of counts below them are equal. The energy scales of both spectra are calibrated at 44.2 keV.

The energy resolution is determined by several contributions. It can be written as

$$R^2 = R_M^2 + R_{nPR}^2 + R_{inh}^2 + R_{tr}^2, \quad (1)$$

where R_M is the contribution from the PMT gain and photon detection Poisson statistics, R_{nPR} is the contribution from the non-proportional response of the scintillator, R_{inh} is the contribution from crystal inhomogeneities, and R_{tr} is the contribution from the transfer of the scintillation photons from the crystal to the PMT.

R_M is given by

$$R_M = 2.35 \sqrt{\frac{1 + \text{var}(M)}{N_{phe}^{PMT}}}, \quad (2)$$

where $\text{var}(M)$ is the fractional variance in the PMT gain, which is 0.27 for the used PMT.¹⁷

Applying Eq. (2) to the number of photoelectrons N_{phe}^{PMT} produced in the PMT, we calculated the values of R_M , see Table II. Because of comparable light yield, R_M contributions are roughly equal for both crystals. The other three contributions are often called the scintillator resolution $R_s = \sqrt{R_{nPR}^2 + R_{inh}^2 + R_{tr}^2}$.¹⁸ The values of R_s derived from Eqs. (1) and (2) are also compiled in Table II. R_s is on average twice smaller in $\text{LaBr}_3:\text{Ce,Sr}$ as compared to that of standard $\text{LaBr}_3:\text{Ce}$. The reason for this significant improvement is either smaller R_{nPR} , R_{inh} , or R_{tr} . Each of them will be further addressed below.

The non-proportionality contribution to the energy resolution originates from the stochastic nature of the ionization track creation. After interaction with matter, an incident γ -ray creates a high-energy electron due to the photoelectric effect, or several high-energy electrons due to multiple Compton scattering events. These primary electron(s) pass through the material, producing ionization track(s). In “head-on” collisions, secondary high-energetic electrons are produced, creating their

TABLE II. Energy resolution (R) derived from pulse-height spectra recorded with various γ -ray and X-ray sources with a R6231-100 PMT and $1\ \mu\text{s}$ amplifier shaping time. R_M and R_s are the values of the PMT and Poisson statistics contribution and the scintillator contribution, respectively.

Source	Target	Energy (keV)	LaBr ₃ :Ce			LaBr ₃ :Ce,Sr		
			R (%)	R_M (%)	R_s (%)	R (%)	R_M (%)	R_s (%)
Amersham variable energy X-ray source	Cu	8.04	35.4	16.4	31.4	26	15.8	20.7
	Rb	13.37	25.4	12.2	22.3	17.3	12.1	12.4
	Mo	17.44	20.1	10.8	16.9	13.9	10.6	9
	Ag	22.1	16.9	9.5	14	11.8	9.4	7.2
	Ba	32.06	13.3	7.8	10.7	9.3	7.8	5.1
	Tb	44.23	12.5	6.6	10.6	8.1	6.6	4.6
²⁴¹ Am		59.5	9.4	5.7	7.5	6.5	5.7	3.2
¹³³ Ba		81	7.7	4.8	6	5.7	4.9	2.8
		276.4	4.2	2.6	3.3	2.9	2.7	1.2
		302.9	3.7	2.5	2.8	2.9	2.5	1.4
		356	3.4	2.3	2.5	2.8	2.4	1.4
	383.9	3.3	2.2	2.5	2.6	2.3	1.3	
²² Na		511	2.8	1.9	2.1	2.4	2	1.4
¹³⁷ Cs		661.7	2.5	1.7	1.8	2	1.7	1.1
⁶⁰ Co		1173	1.9	1.2	1.3	1.5	1.3	0.8
		1332	1.8	1.2	1.5	1.4	1.2	0.7

own ionization tracks. All these processes are probabilistic: the amount and energies of the primary and secondary electrons vary from event to event. For all known materials, the scintillation response is not proportional to the incident electron energy.^{19–22} The total γ -ray response thus varies from event to event broadening the full absorption peak. In Ref. 11, we showed that the electron response is remarkably more proportional in LaBr₃:Ce,Sr as compared to standard LaBr₃:Ce. This results in a much smaller contribution of R_{nPR} and an improved energy resolution in LaBr₃:Ce,Sr.

The remaining contributions R_{tr} and R_{inh} are most likely not affected by Sr co-doping. Both, LaBr₃:Ce and LaBr₃:Ce,Sr crystal pieces had quite similar size and shape, the crystals were grown with the same technique and the pulse-height spectra were recorded under the same experimental conditions. This again supports our assumption that R is improved in LaBr₃:Ce,Sr due to a considerably reduced contribution of the non-proportionality R_{nPR} .

B. Scintillation properties of LaBr₃:Ce co-doped with Li, Na, Mg, Ca, Sr, and Ba

In Ref. 11, we showed that LaBr₃:Ce,Sr has a more proportional response to 10–100 keV X-rays as compared to standard LaBr₃:Ce. To verify whether other co-dopants have similar effects on the proportionality, we studied the scintillation response to γ -ray energies between 8 keV and 1.33 MeV using a standard set of radioactive sources, see Fig. 4. The responses of Li, Na, and Mg co-doped samples do not show a significant difference as compared the standard LaBr₃:Ce. Scintillation responses of Ca, Sr, and Ba co-doped crystals are considerably more proportional. The most prominent effect is observed at energies below 100 keV. The proportionality of the LaBr₃:Ce response drops below 90% at 8 keV.

The proportionality of Sr and Ba co-doped LaBr₃:Ce are still above 95% at 8 keV, and that of the Ca co-doped crystal is above 100% for the entire studied γ -ray energy range. The proportionalities of group A and group B crystals of LaBr₃:Ce,Sr coincide within the error, which indicates that the proportionality improvement is reproducible.

Compared to group A LaBr₃:Ce, group A LaBr₃:Ce,Li crystal has a slightly higher light yield, but the same energy resolution, see Table III. This is not a surprising result, since the proportionality of LaBr₃:Ce,Li is the same as in standard LaBr₃:Ce, see Fig. 4.

All co-doped group B crystals showed a 10%–20% higher light yield as compared to group B standard LaBr₃:Ce. The Na co-doped sample provides a better energy resolution.

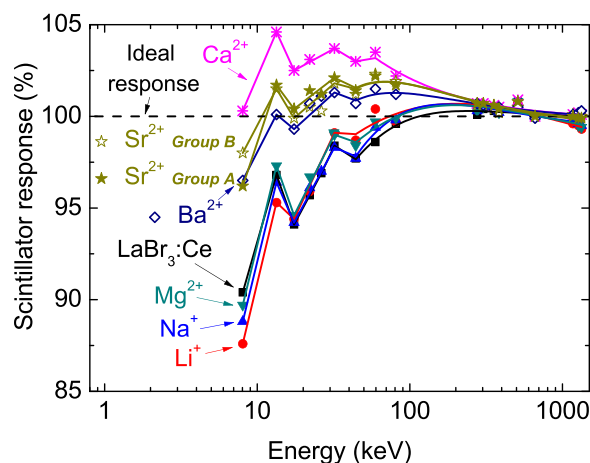


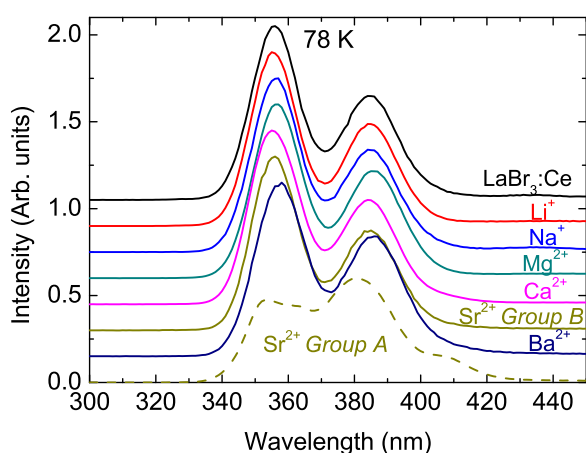
FIG. 4. Scintillator response as a function of absorbed γ -ray energy normalized to 100% at 662 keV. Lines are drawn to guide the eye. The errors are within 2%–3% below 10 keV, within 1%–2% in the 10–30 keV range, and <1% above 30 keV.

TABLE III. Light yield and energy resolution (R) of LaBr₃:Ce with different co-dopants derived from pulse-height spectra recorded under ²⁴¹Am and ¹³⁷Cs γ -ray excitation with a bialkali R1791 PMT. The values of the light yield in column 4 are relative to the yield of group B LaBr₃:Ce crystals.

Crystals	Co-dopant	Light yield at 662 keV (ph/MeV)	Relative yield	R (% at 662 keV)	R (% at 60 keV)	R (% at 32 keV)
Group B LaBr ₃ :Ce	...	64 000	1	3.1	10.6	15.6
	Na ⁺	73 000	1.14	2.7	10	14.8
	Mg ²⁺	73 000	1.14	3.0	10.6	15.4
	Ca ²⁺	71 000	1.11	2.9	8.2	11.5
	Sr ²⁺	76 000	1.19	2.8	8.6	13.3
	Ba ²⁺	69 000	1.08	3.7	10.2	15.3
Group A LaBr ₃ :Ce	...	76 000	1.19	2.7	10.7	14.6
	Li ⁺	78 000	1.22	2.7	10.8	14.6
	Sr ²⁺	78 000	1.22	2.35	7.8	11.7

Since its proportionality is the same as that of standard LaBr₃:Ce, this improvement is ascribed either to a higher light yield or a better crystal quality of LaBr₃:Ce,Na. The Mg co-doped crystal has a higher light yield; however, its energy resolution does not improve. Both Ca and Sr co-doped samples showed a better energy resolution as compared to standard LaBr₃:Ce. This agrees with their higher light yield and improved proportionality. The Ca co-doped sample showed an impressively low value of the energy resolution of 11.5% at 32 keV, which is better than that of all other studied samples. This is ascribed to the most efficient scintillation response of LaBr₃:Ce,Ca among all the studied samples at energies below 60 keV, see Fig. 4. The Ba co-doped crystal has a worse resolution at 662 keV but is better at energies below 60 keV. Considering the improved proportionality and higher light yield, one could expect a better performance at all energies as compared to the standard LaBr₃:Ce. Apparently, the crystal quality affects the energy resolution in this particular Ba co-doped LaBr₃:Ce crystal. Yang *et al.*² reported a better energy resolution in Ba co-doped LaBr₃:Ce as compared to the standard material.

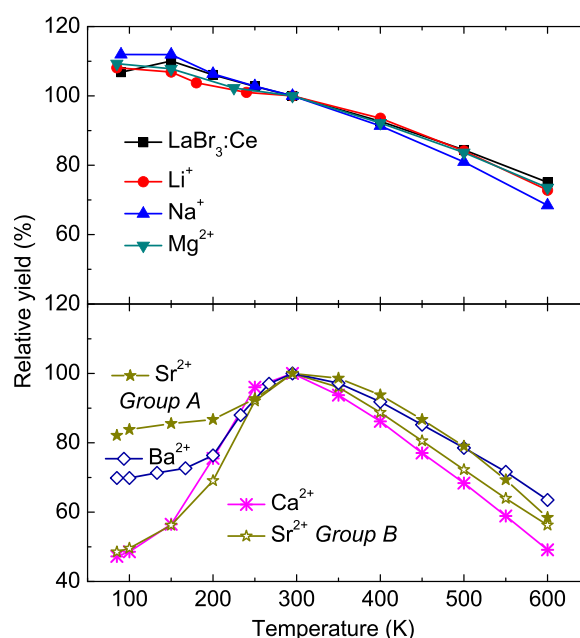
Note that the values of the energy resolution obtained with a R6231-100 PMT and compiled in Table II are lower than those obtained with a R1791 PMT and compiled in Table III. The R6231-100 PMT has a $\sim 50\%$ higher quantum efficiency than the R1791 and, therefore, a lower contribution of R_M to the total energy resolution R. Group B crystals

FIG. 5. X-ray excited emission spectra of standard LaBr₃:Ce and LaBr₃:Ce co-doped crystals with Li, Na, Mg, Ca, Sr, and Ba recorded at 78 K.

show a worse light yield and energy resolution as compared to group A crystals. Apparently, this is due to the crystal quality or crystal growth process. Better quality Ca and Ba co-doped LaBr₃:Ce crystals have therefore a potential to show similar or even better values of energy resolution than those of the LaBr₃:Ce,Sr samples compiled in Table II.

Fig. 5 shows the X-ray excited emission spectra of the co-doped LaBr₃:Ce crystals at 78 K. All the samples show the typical double-band Ce³⁺ 5d-4f emission with maxima at 355 nm and 385 nm according to the transitions into the ²F_{5/2} and ²F_{7/2} states, respectively. Group A LaBr₃:Ce,Sr spectrum is different. It has additional bands that are apparently emissions from perturbed Ce³⁺ sites.

Fig. 6 shows the photoelectron yield of the studied LaBr₃:Ce crystals as a function of temperature normalized to 100% at 295 K. The yield was derived from pulse-height spectra on samples in the cryostat recorded with a 10 μ s shaping time under ¹³⁷Cs 662 keV γ -ray excitation. The temperature dependences of Li, Na, and Mg co-doped samples are similar to that of standard LaBr₃:Ce. The yield

FIG. 6. Temperature dependence of the relative photoelectron yield of standard LaBr₃:Ce and LaBr₃:Ce co-doped samples with Li, Na, Mg, Ca, Sr, and Ba. The spectra are normalized to 100% at 295 K.

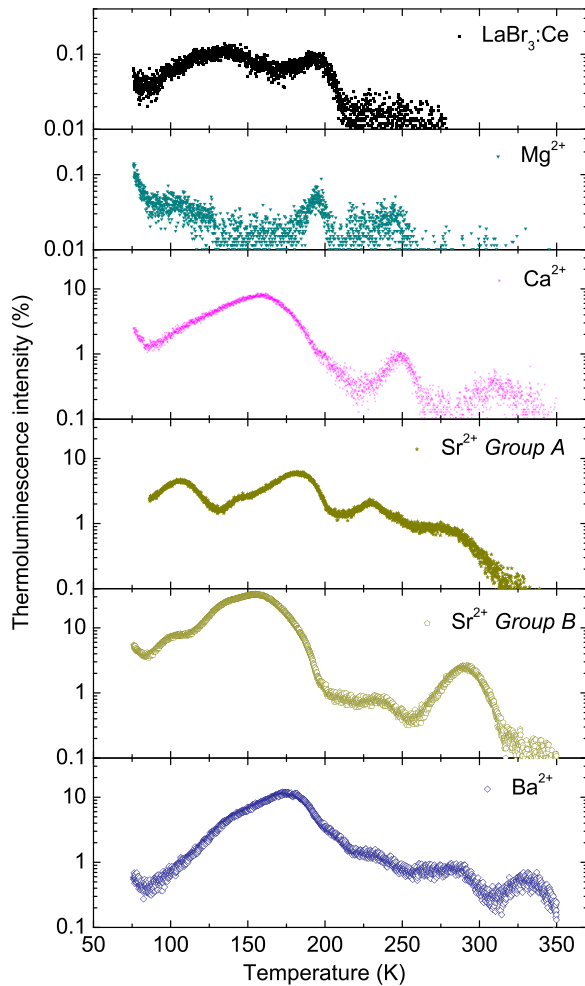


FIG. 7. Thermoluminescence glow curves of $\text{LaBr}_3:\text{Ce}$ and $\text{LaBr}_3:\text{Ce}$ co-doped samples with Mg, Ca, Sr, and Ba. The curves are normalized to the SSL at 78 K.

continuously decreases from 110% at 85 K to 70%–75% at 600 K. The temperature dependences of Ca, Sr, and Ba co-doped $\text{LaBr}_3:\text{Ce}$ crystals are different. The yield of those samples is maximal at room temperature. At 85 K, it decreases to 50%–80%. Above 295 K, the yield decreases to 50–65%.

To further study the origin of the light yield decrease at temperatures below 295 K, thermoluminescence measurements were performed. Fig. 7 shows thermoluminescence

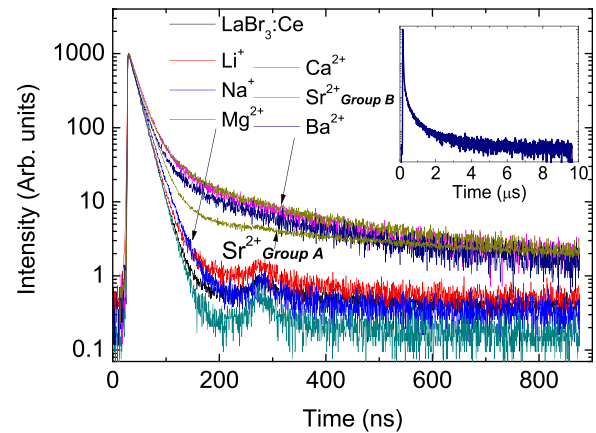


FIG. 8. Scintillation decay profiles of 1.5–3 mm thick $\text{LaBr}_3:\text{Ce}$ and $\text{LaBr}_3:\text{Ce}$ co-doped crystals with Li, Na, Mg, Ca, Sr, and Ba recorded under ^{137}Cs γ -ray excitation monitoring the 350–420 nm emission at 295 K. The inset shows the scintillation decay curve of group B $\text{LaBr}_3:\text{Ce,Ba}$ sample on a shorter time scale.

glow curves of the studied samples. Multiple peaks were observed on the Ca, Sr, and Ba co-doped $\text{LaBr}_3:\text{Ce}$ spectra below 350 K. The maximal thermoluminescence emission intensities of these samples are $\sim 10\%$ – 30% of their steady-state X-ray excited luminescence intensities (SSL). For comparison, the maximal thermoluminescence emission intensities of standard and Mg co-doped $\text{LaBr}_3:\text{Ce}$ samples are two orders of magnitude lower. The thermoluminescence glow spectra of Li and Na co-doped samples could not even be distinguished from the background noise.

The thermoluminescence glow peaks are caused by the release of trapped charge carriers. Their concentration in Ca, Sr, and Ba co-doped samples is considerably higher than in standard $\text{LaBr}_3:\text{Ce}$. The release of trapped charge carriers results in phosphorescence decay components²³ which last much longer than the 10 μs electronic shaping time used in the photoelectron yield measurements. Therefore, these components do not contribute to the photoelectron yield.

Scintillation decay profiles of the co-doped $\text{LaBr}_3:\text{Ce}$ crystals recorded under ^{137}Cs γ -ray excitation are shown in Fig. 8. The decay profiles were fit with several exponential functions, see Table IV. Standard and Li, Na, and Mg co-doped $\text{LaBr}_3:\text{Ce}$ samples have single-exponential decays with decay times of 15–16.5 ns. Decay profiles of Ca, Sr, and Ba co-doped $\text{LaBr}_3:\text{Ce}$ are different. First, they have longer

TABLE IV. Scintillation decay time components of standard $\text{LaBr}_3:\text{Ce}$ and $\text{LaBr}_3:\text{Ce}$ co-doped crystals with Li, Na, Mg, Ca, Sr, and Ba and their relative contributions to the total scintillation output.

$\text{LaBr}_3:\text{Ce}^{3+}$ co-doped with	Thickness, mm^3	Components			
		Fast (ns)	Slow I (ns)	Slow II (ns)	Slow III (ns)
...	1.5	15.1 (100%)
Li^+	3	15.5 (100%)
Na^+	3	16.7 (100%)
Mg^{2+}	2.5	15.2 (100%)
Ca^{2+}	1.5	17.6 (62%)	55 (15%)	220 (14%)	1210 (9%)
Sr^{2+} group A	3	18.2 (78%)	82 (3%)	470 (11%)	2500 (8%)
Sr^{2+} group B	2	16.8 (56%)	56 (16%)	240 (16%)	1530 (12%)
Ba^{2+}	1.5	16.5 (64%)	75 (15%)	360 (13%)	2250 (8%)

Ce³⁺ emission decay time constants of 16.5–18 ns. The longer decay times were also observed in Sr and Ba co-doped LaBr₃:Ce.¹² Second, Ca, Sr, and Ba co-doped LaBr₃:Ce have additional μ s-long decay components, which contain 20%–45% of the total light output. Apparently, these components are due to phosphorescence from the slow release of trapped charge carriers.

IV. SUMMARY AND CONCLUSION

LaBr₃:5%Ce crystals co-doped with Li, Na, Mg, Ca, Sr, and Ba were grown at two different institutes and their scintillation properties were evaluated. Measured with a R6231–100 PMT, the energy resolution of Sr co-doped LaBr₃:5%Ce crystals showed record low values, for example, 2% at 662 keV, 6.5% at 59.5 keV, and 9.3% at 32 keV.

The light yield of each studied co-doped sample is higher as compared to standard LaBr₃:Ce. The energy resolution of LaBr₃:Ce improves with Na, Ca, and Sr co-doping. The proportionality improves with Ca, Sr, and Ba co-doping. Apart from this, the Ca, Sr, and Ba co-doped samples have μ s-long decay time components, their light yield decreases at temperatures below 295 K, and multiple thermoluminescence glow peaks are observed below 350 K. These properties are ascribed to the presence of charge carrier traps in Ca, Sr, and Ba co-doped samples.

ACKNOWLEDGMENTS

This work was funded by the Dutch Technology Foundation (STW) and Saint Gobain Crystals, France. The authors acknowledge Vladimir Ouspenski, Francesco Quarati, and Johan de Haas for useful discussions.

¹E. V. D. van Loef, P. Dorenbos, C. W. E. van Eijk, K. Krämer, and H. U. Güdel, *Appl. Phys. Lett.* **79**, 1573 (2001).

²A. Iltis, M. R. Mayhugh, P. Menge, C. M. Rozsa, O. Selles, and V. Solov'yev, *Nucl. Instrum. Methods Phys. Res. A* **563**, 359 (2006).

³K. S. Shah, J. Glodo, M. Klugerman, W. W. Moses, S. E. Derenzo, and M. J. Weber, *IEEE Trans. Nucl. Sci.* **50**, 2410 (2003).

⁴A. Kuhn, S. Surti, J. S. Karp, P. S. Raby, K. S. Shah, A. E. Perkins, and G. Muehllehner, *IEEE Trans. Nucl. Sci.* **51**, 2550 (2004).

⁵D. R. Schaart, S. Seifert, R. Vinke, H. T. van Dam, P. Dendooven, H. Lohner, and F. J. Beekman, *Phys. Med. Biol.* **55**, N179 (2010).

⁶A. Owens, A. J. J. Bos, S. Brandenburg, E. J. Buis, C. Dathy, P. Dorenbos, C. W. E. van Eijk, S. Kraft, R. W. Ostendorf, V. Ouspenski, and F. Quarati, *Nucl. Instrum. Methods Phys. Res. A* **572**, 785 (2007).

⁷F. G. A. Quarati, A. Owens, P. Dorenbos, J. T. M. de Haas, G. Benzoni, N. Blasi, C. Boiano, S. Brambilla, F. Camera, R. Alba, G. Bellia, C. Maiolino, D. Santonocito, M. Ahmed, N. Brown, S. Stave, H. R. Weller, and Y. K. Wu, *Nucl. Instrum. Methods Phys. Res. A* **629**, 157 (2011).

⁸Saint-Gobain Technical Note, "BrilLanCe Scintillators: Performance Summary," 2009.

⁹I. Mazumdar, D. A. Gothe, G. Anil Kumar, N. Yadav, P. B. Chavan, and S. M. Patel, *Nucl. Instrum. Methods Phys. Res. A* **705**, 85 (2013).

¹⁰R. Pani, M. N. Cinti, R. Pellegrini, P. Bennati, M. Betti, F. Vittorini, M. Mattioli, G. Trotta, V. Orsolini Cencelli, R. Scafe, F. Navarra, D. Bollini, G. Baldazzi, G. Moschini, and F. de Notaristefani, *Nucl. Instrum. Methods Phys. Res. A* **576**, 15 (2007).

¹¹M. S. Alekhin, J. T. M. de Haas, I. V. Khodyuk, K. W. Krämer, P. R. Menge, V. Ouspenski, and P. Dorenbos, *Appl. Phys. Lett.* **102**, 161915 (2013).

¹²K. Yang, P. R. Menge, J. J. Buzniak, and V. Ouspenski, in *Nuclear Science Symposium and Medical Imaging Conference*, Anaheim (California, 2012), p. 308.

¹³P. Dorenbos, J. T. M. de Haas, and C. W. E. van Eijk, *IEEE Trans. Nucl. Sci.* **51**, 1289 (2004).

¹⁴J. T. M. de Haas and P. Dorenbos, *IEEE Trans. Nucl. Sci.* **55**, 1086 (2008).

¹⁵L. M. Bollinger and G. E. Thomas, *Rev. Sci. Instrum.* **32**, 1044 (1961).

¹⁶G. Bizzarri, J. T. M. de Haas, P. Dorenbos, and C. W. E. van Eijk, *Phys. Status Solidi A* **203**, R41(2006).

¹⁷J. T. M. de Haas and P. Dorenbos, *IEEE Trans. Nucl. Sci.* **58**, 1290 (2011).

¹⁸P. Dorenbos, J. T. M. de Haas, and C. W. E. van Eijk, *IEEE Trans. Nucl. Sci.* **42**, 2190 (1995).

¹⁹S. A. Payne, W. W. Moses, S. Sheets, L. Ahle, N. J. Cherepy, B. Sturm, S. Dazeley, G. Bizzarri, and C. Woon-Seng, *IEEE Trans. Nucl. Sci.* **58**, 3392 (2011).

²⁰I. V. Khodyuk, J. T. M. de Haas, and P. Dorenbos, *IEEE Trans. Nucl. Sci.* **57**, 1175 (2010).

²¹I. V. Khodyuk, P. A. Rodnyi, and P. Dorenbos, *J. Appl. Phys.* **107**, 113513 (2010).

²²I. V. Khodyuk and P. Dorenbos, *J. Phys.: Condens. Matter* **22**, 485402 (2010).

²³J. T. Randall and M. H. F. Wilkins, *Proc. R. Soc. London* **184**, 365 (1945).